



Cerebellar Volumetry in Ataxias: Relation to Ataxia Severity and Duration

Mónica Ferreira¹ · Tamara Schaprian¹ · David Kügler¹ · Martin Reuter^{1,2,3} · Katharina Deike-Hoffmann⁴ · Dagmar Timmann⁵ · Thomas M. Ernst⁵ · Paola Giunti^{6,7} · Hector Garcia-Moreno^{6,7} · Bart van de Warrenburg⁸ · Judith van Gaalen^{8,9} · Jeroen de Vries¹⁰ · Heike Jacobi¹¹ · Katharina Marie Steiner⁵ · Gülin Öz¹² · James M. Joers¹² · Chiadi Onyike¹³ · Michal Povazan¹³ · Kathrin Reetz^{14,15} · Sandro Romanzetti¹⁴ · Thomas Klockgether^{1,16} · Jennifer Faber^{1,16}

Accepted: 15 January 2024
© The Author(s) 2024

Abstract

Cerebellar atrophy is the neuropathological hallmark of most ataxias. Hence, quantifying the volume of the cerebellar grey and white matter is of great interest. In this study, we aim to identify volume differences in the cerebellum between spinocerebellar ataxia type 1 (SCA1), SCA3 and SCA6 as well as multiple system atrophy of cerebellar type (MSA-C). Our cross-sectional data set comprised mutation carriers of SCA1 (N=12), SCA3 (N=62), SCA6 (N=14), as well as MSA-C patients (N=16). Cerebellar volumes were obtained from T1-weighted magnetic resonance images. To compare the different atrophy patterns, we performed a z-transformation and plotted the intercept of each patient group's model at the mean of 7 years of ataxia duration as well as at the mean ataxia severity of 14 points in the SARA sum score. In addition, we plotted the extrapolation at ataxia duration of 0 years as well as 0 points in the SARA sum score. Patients with MSA-C demonstrated the most pronounced volume loss, particularly in the cerebellar white matter, at the late time intercept. Patients with SCA6 showed a pronounced volume loss in cerebellar grey matter with increasing ataxia severity compared to all other patient groups. MSA-C, SCA1 and SCA3 showed a prominent atrophy of the cerebellar white matter. Our results (i) confirmed SCA6 being considered as a pure cerebellar grey matter disease, (ii) emphasise the involvement of cerebellar white matter in the neuropathology of SCA1, SCA3 and MSA-C, and (iii) reflect the rapid clinical progression in MSA-C.

Keywords Ataxia · Atrophy · Cerebellum · z-scores

Introduction

Among the adult-onset degenerative cerebellar ataxias, the autosomal dominantly inherited polyglutamine spinocerebellar ataxias type 1 (SCA1), SCA3, and SCA6, and the sporadic multiple system atrophy of cerebellar type (MSA-C) are most common [1]. SCA1, SCA3 and SCA6 are caused by translated CAG repeat expansion mutations of variable length in the respective genes. The mutations result in formation of abnormal disease proteins containing elongated polyglutamine stretches [1]. MSA-C is neuropathologically defined by the presence of alpha-synuclein-positive inclusions in oligodendroglia. The diagnosis of MSA-C relies on

clinical features, particularly including severe autonomic failure [2, 3]. SCA1, SCA3, and MSA-C are multisystemic diseases that not only affect the cerebellum, but also involve the spinal cord, brainstem, basal ganglia, and other regions of the central nervous system. Ataxia is the primary clinical feature, with additional other non-ataxia symptoms such as spasticity, rigidity or ophthalmoparesis. In contrast, SCA6 is considered as an almost purely cerebellar disease characterised by isolated cerebellar ataxia without major non-ataxia signs [1, 4]. Previous neuropathological and MRI studies examining the atrophy patterns of SCA1, SCA3, SCA6, and MSA-C have, to date, predominantly used voxel-based morphometry and emphasised the involvement of extracerebellar structures [5–11]. While voxel-wise analysis can be useful for detecting subtle or widespread changes in brain structure, it is essential to focus on specific regions of the cerebellum when studying cerebellar ataxias. Recent progress in the MRI

✉ Jennifer Faber
jennifer.faber@dzne.de

Extended author information available on the last page of the article

morphometric analysis of the cerebellum allows detailed quantitative assessment of the cerebellum at the lobular level and precise delineation of cerebellar white matter [12].

The aim of this study was the investigation of the pattern of cerebellar grey and white matter atrophy in SCA1, SCA3, SCA6 and MSA-C. We applied a z-transformation to correct for age effects and used a linear model with read-outs at defined time points of the disease course and degrees of ataxia severity, to allow the comparison of the amount and pattern of cerebellar atrophy between SCA1, SCA3, SCA6 and MSA-C.

Methods

Participants

Cross-sectional data of SCA1 ($N = 12$), SCA3 ($N = 62$), SCA6 ($N = 14$) and MSA-C ($N = 16$) were analysed. In addition, healthy controls (HCs) ($N = 292$) were analysed and used as a reference for the z-transformation. All subjects participated in ongoing observational studies (ESMI, SCA Registry, DANCER, DELCODE) at 8 European and 2 US sites, and were enrolled between 2017 and 2022. All participants gave their written informed consent according to the declaration of Helsinki. SCA diagnosis was confirmed by diagnostic genetic testing, MSA-C was diagnosed applying the diagnostic criteria from 2008 [2]. The new diagnostic criteria of Wenning et al. [3] could not be applied retrospectively. Ataxia severity was assessed using the Scale of Assessment and Rating of Ataxia (SARA) [13]. We only included ataxic patients with SARA sum scores higher than

or equal to the established cutoff value of 3 [13, 14]. Ataxia onset was defined as the first occurrence of gait disturbances, and the reported ataxia duration in years was calculated accordingly.

Imaging Protocol

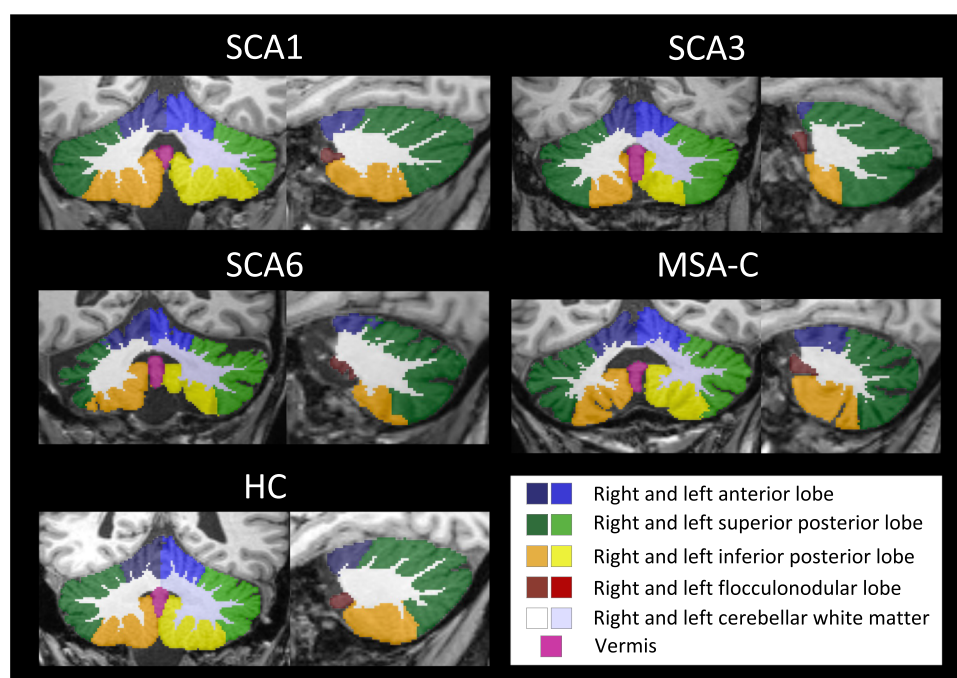
All participants were scanned on 3T SIEMENS scanners, with a 32-channel head coil, using a standardised T1-weighted magnetisation-prepared rapid gradient-echo (MPRAGE) sequence. Sequence parameters were as follows: repetition time (TR) = 2500 ms, echo time (TE) = 4.37 ms, inversion time (TI) = 1100 ms, flip angle = 7°, field of view 256 x 256 mm² and 192 slices, voxel size = 1 mm isotropic.

Image Analysis

We used *CerebNet* [12] for the automated sub-segmentation of the cerebellum into the following volumes (for hemispheric volumes, each volume corresponds to the combined volumes of left and right hemisphere): anterior lobe (consisting of the lobules I-V), superior posterior lobe (consisting of the lobules VI-VII), inferior posterior lobe (consisting of the lobules VIII-IX) and the flocculonodular lobe (corresponding to lobule X) and the midline vermis as well as the cerebellar white matter (cWM). In addition we analysed the combined volume of cerebellar grey matter (cGM) comprised of all hemispheric volumes plus vermis. All scans were visually inspected.

Exemplary cases of the automated cerebellar segmentations are shown in Fig. 1.

Fig. 1 Segmentation examples of a fully automated cerebellar segmentation in SCA1, SCA3, SCA6 and MSA-C patients as well as in a HC, projected onto a coronal and sagittal slice



To account for individual differences in head size, we used estimated total intracranial volume (eTIV) calculated with *FreeSurfer* (version 6.0.0) [15]. Normalised cerebellar volumes were calculated by dividing the raw cerebellar volumes by the individual's eTIV. These values were harmonised across sites using the ComBat method to adjust for potential batch effects [16–18].

Statistical Analysis of Cerebellar Atrophy in Relation to Ataxia Duration and Ataxia Severity

All statistical analyses were performed using R Software for Statistical Computing, version 4.2.3 [19]. In order to compare volumes across the different diseases, we z-transformed each normalised volume in relation to HCs to compensate for age-related atrophy, as described previously [20]. Here, a z-score of 0 corresponds to the respective, expected mean in HCs of the same age. A z-score of ± 1 , ± 2 etc. corresponds to ± 1 , ± 2 etc. standard deviations below or above the expected mean in HCs of the same age [20]. The resulting z-scores were used for all subsequent statistical analyses.

In order to compare the different ataxias at the same time points of ataxia duration and degrees of ataxia severity the following stepwise approach was performed for each considered cerebellar volume. First, we plotted the z-scores for each cerebellar volume against the reported ataxia duration in years as well as ataxia severity assessed with the SARA sum score. Here, we applied a linear model for each disease and calculated the coefficient of determination (R^2) and p-value for every correlation. Moreover, quadratic and cubic models were also established. Second, we defined the points for comparison: (i) we calculated the overall mean ataxia duration and ataxia severity for all patient groups, which were 7 years of ataxia duration and a SARA sum score of 14, and (ii) we used the extrapolation at 0 years of ataxia duration and the absence of ataxia (SARA sum score of 0). Accordingly, the intercept volume z-score of the linear interpolation line at 0 years and 7 years of ataxia duration, and at a SARA sum score of 0 and 14, were extracted for each disease. Finally, radar plots of these intercept z-scores for each considered volume were used to visualise the degree and patterns of cerebellar

atrophy in SCA1, SCA3, SCA6 and MSA-C at 0 and 7 years of disease duration as well as an ataxia severity of 0 and 14 points in the SARA sum score.

Results

Demographic and characterising data are summarised in Table 1. SCA1 had the earliest age of onset, while SCA3 patients the longest reported ataxia duration, followed by SCA6. Notably, MSA-C was associated with the highest SARA sum scores among all studied ataxia groups.

Cerebellar Atrophy in Relation to Ataxia Duration and Ataxia Severity

The linear model of volume z-scores and ataxia duration as well as severity are given in Figs. 2 and 3. The coefficient of determination (R^2) as well as the p-value representing evidence of a linear relationship are given in the superior left corner of each subplot. Using quadratic and cubic models, neither the residual versus fitted values plots nor the Q-Q plots showed substantial improvement in comparison to the linear model. Thus, given the limited sample size we based the further analyses on the linear model (Supplement Figs. 4–15).

The relation of cerebellar volumes and ataxia duration in years is shown in Fig. 2. Overall, most volumes decreased with increased ataxia duration. The steepest decline of all cerebellar grey and white matter volumes was observed in MSA-C, followed by SCA6 except for cerebellar white matter. In SCA1, the anterior, superior posterior, and flocculonodular lobe, and in SCA3 the anterior, superior posterior and flocculonodular lobe as well as aggregated cGM, showed a not significant slight volume increase with longer ataxia duration.

With regard to ataxia severity, most volumes decreased with increased ataxia severity. Overall, MSA-C and SCA6 showed the steepest decline in all grey matter volumes, and MSA-C additionally in the white matter volume, with exception for cWM in SCA6 that presented a slight volume

Table 1 Demographic and cohort characteristics

Group entity	Number (Female/ Male)	Age at scan ¹ mean (SD)	Ataxia duration mean (SD)	SARA sum score mean (SD)	CAG repeats ² mean (SD)
SCA1	12 (7/5)	45.1 (9.6)	3.9 (3.3)	12.1 (3.9)	48.3 (4.2)
SCA3	62 (25/37)	50.7 (10.6)	10.8 (6.5)	12.8 (6.2)	67.8 (8.0)
SCA6	14 (4/10)	64.2 (8.6)	7.8 (5.5)	13.3 (4.9)	21.8 (0.5)
MSA-C	16 (6/10)	64.5 (8.2)	4.4 (2.1)	17.2 (5.2)	n.a.
HC	292 (160/132)	63.5 (12.6)	n.a.	n.a.	n.a.

SD, standard deviation; SCA, spinocerebellar ataxia; MSA-C, multiple system atrophy of cerebellar type; HC, healthy control; n.a., not applicable. ¹ in years; ² of the longer allele

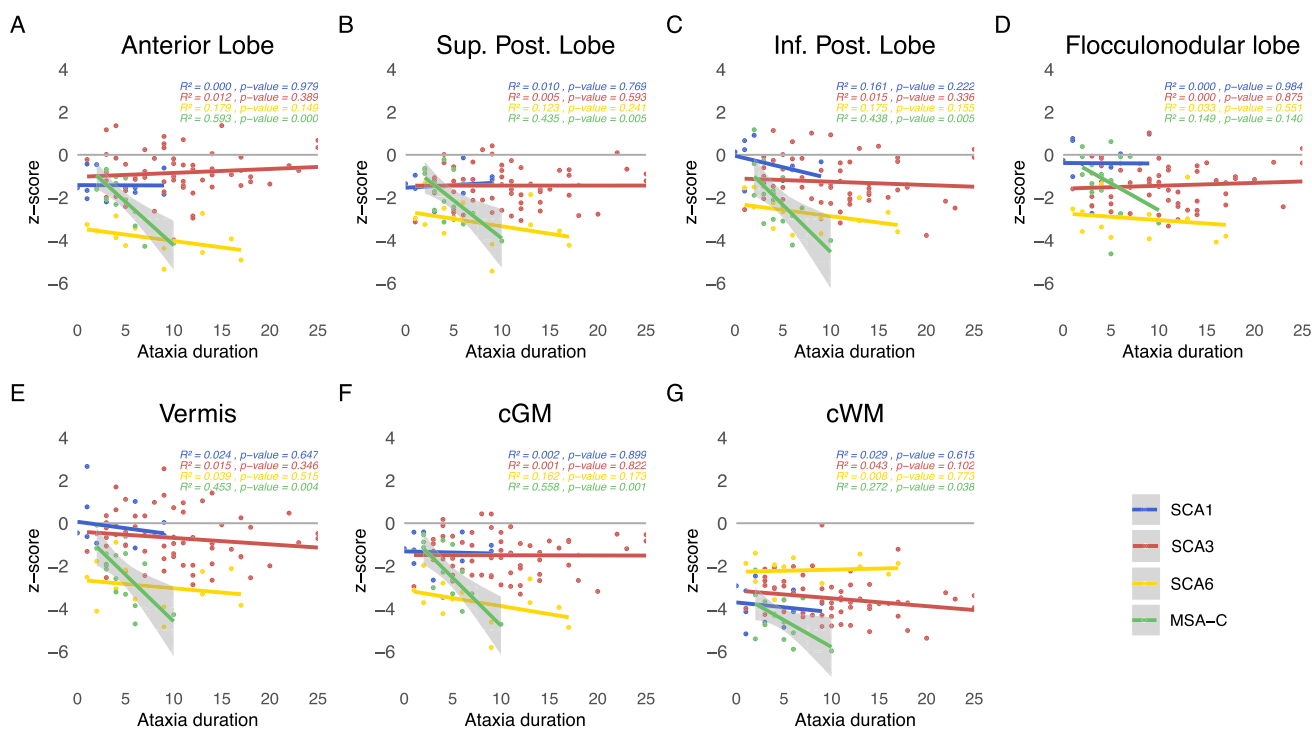


Fig. 2 Relation of cerebellar volumes and ataxia duration in years. The z-scores of each cerebellar sub-segmented region are plotted against the reported ataxia duration in years for SCA1 (in blue), SCA3 (in red), SCA6 (in yellow) and MSA-C (in green). Linear interpolation

was applied with the 95% confidence intervals given as shaded grey areas for linear regressions with significant correlations ($p \leq 0.05$). Values of the coefficient of determination (R^2) as well as the p-value are given for each disease, respectively

increase. In SCA1 the anterior and superior posterior lobe, as well as cGM, and in SCA3 the flocculonodular lobe and the vermis, as well as in SCA6 the cerebellar white matter showed a not significant slight volume increase with increased ataxia severity. The relation between cerebellar volumes and ataxia severity is shown in Fig. 3.

R^2 values were overall relatively small, and ranged between 0 and 0.54. Generally, the highest R^2 was observed in MSA-C followed by SCA6. In MSA-C R^2 was emphasised in relation to ataxia duration with the maximum of $R^2 = 0.537$ for cGM. In SCA6 R^2 was emphasised in relation to ataxia severity. SCA1 and SCA3 showed very small values of R^2 , except for the relation of cWM and ataxia severity in SCA3. In MSA-C the correlation with ataxia duration of all cerebellar volumes reached statistical significance with $p \leq 0.05$, except for the flocculonodular lobe. The correlation with ataxia severity reached statistical significance in all volumes, except the anterior lobe and vermis and MSA-C. In the SCAs, only the correlation of cerebellar white matter and ataxia severity in SCA3 reached statistical significance with a $p \leq 0.05$.

To visualise for each disease the pattern and extent of atrophy at certain time points of ataxia duration and degrees of ataxia severity, we displayed the linear interpolated z-scores for the volumes of the anterior, superior posterior and inferior

posterior and flocculonodular lobe and vermis as well as cGM and cWM in radar plots. Figure 4 shows radar plots of the extrapolation at the time of ataxia onset (ataxia duration of 0 years) and at 7 years after ataxia onset, as well as for the intercept at SARA sum scores of 0 and 14. Comparison of the radar plots at ataxia onset and at 7 years after onset revealed a strong atrophy increase in MSA-C, whereas the increase was less pronounced in the SCAs. Comparison of the plots at SARA sum score of 0 and of 14 revealed an emphasised atrophy increase in SCA6 and MSA-C, whereas the increase was only minor in SCA1 and SCA3. Moreover, in SCA1, SCA3 and MSA-C cWM volume was consistently affected, in contrast to SCA6, where the cWM was considerably less affected than the grey matter structures.

Discussion

We used a z-transformation to study the degree and distribution of cerebellar atrophy in SCA1, SCA3, SCA6 and MSA-C at certain levels of ataxia duration and ataxia severity, while accounting for the healthy aging effect. We could demonstrate a strong coherence between ataxia severity and grey matter atrophy in SCA6, underlining the consideration of SCA6 as a pure cerebellar disease. In contrast, volume loss of

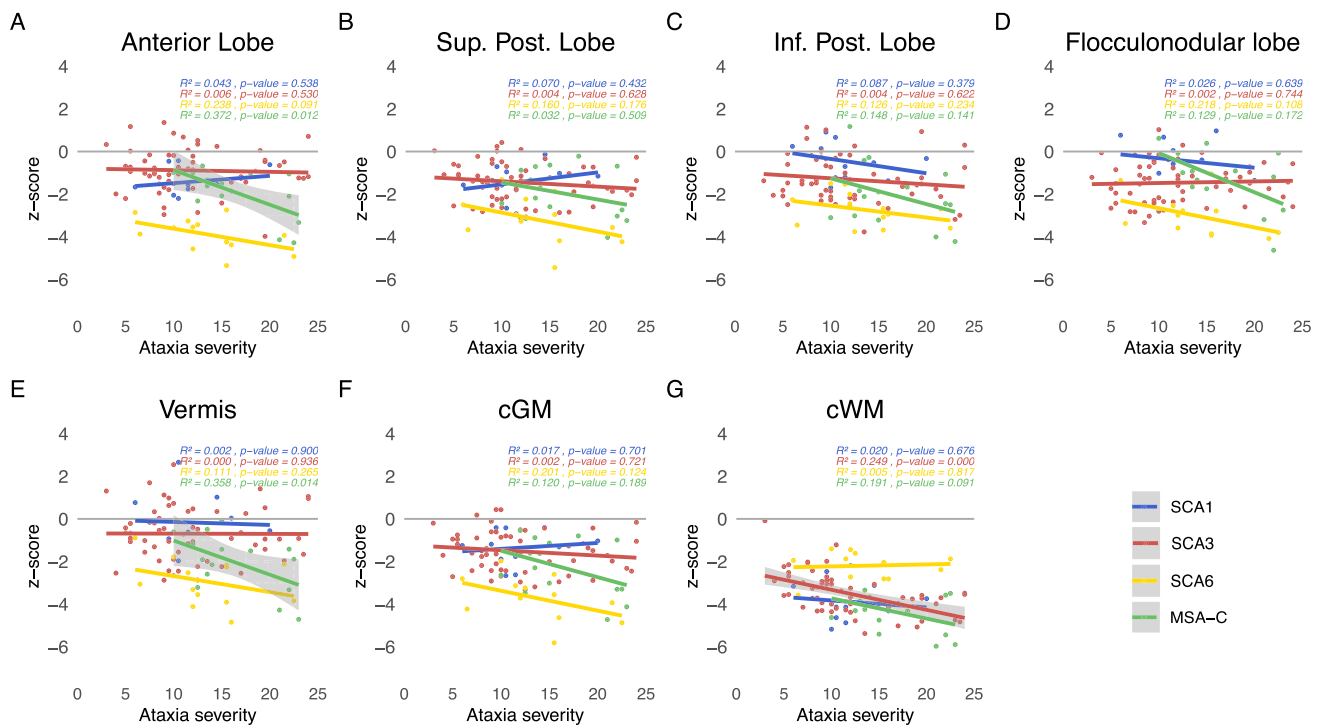


Fig. 3 Relation of cerebellar volumes and ataxia severity. The z-scores of each cerebellar sub-segmented region are plotted against ataxia severity measured with SARA sum score for SCA1 (in blue), SCA3 (in red), SCA6 (in yellow) and MSA-C (in green). Linear interpolation

was applied with the 95% confidence intervals given as shaded grey areas for linear regressions with significant correlations ($p \leq 0.05$). Values of the coefficient of determination (R^2) as well as the p-value are given for each disease, respectively

the cerebellar white matter was prominent in MSA-C, SCA1 and SCA3. Overall MSA-C showed the steepest decline of all cerebellar white and grey matter volumes in particular in relation to ataxia duration.

Since ataxias are rare diseases, patient populations are often small and additionally, as in our sample, differ in duration and severity of ataxia, making comparison between entities difficult. We chose the applied approach to overcome this limitation and used radar plots to visualise the differences in atrophy patterns between diseases at certain levels of ataxia duration and severity.

Our results are in line with previous studies mainly of voxel-based-morphometry as well as volumetry in SCAs and MSA-C [5, 6, 8, 21–23]. Notably, throughout the different considered intersections of ataxia duration and ataxia severity, we confirmed earlier findings that, in contrast to other SCA genotypes, atrophy in SCA6 was mainly restricted to the cerebellar GM almost excluding the WM [24, 25]. While cerebellar GM atrophy at the extrapolated point of 0 SARA sum score has no clear discernible pattern across the diseases, it becomes markedly emphasised in SCA6 with increasing ataxia severity in comparison to SCA1, SCA3 and MSA-C. Thus, in SCA6 cerebellar atrophy seems to account almost solely for the clinically observed ataxia. In contrast, it is known, that the neuropathology in the other, multisystemic

disorders SCA1, SCA3 and MSA-C also involves other parts of the central nervous system, e.g. brainstem and basal ganglia [1, 20, 26]. Here, the resulting non-ataxia symptoms, e.g. spasticity or rigidity, probably exacerbate motor and coordination impairments. In other words, by concept, the impairments measured by the SARA scale primarily capture ataxia but may be aggravated by other non-ataxia symptoms. With regard to ataxia duration, MSA-C shows the most pronounced cerebellar grey and white matter atrophy with increasing ataxia duration. This observation reflects the known rapid clinical progression in MSA-C [27]. For the clinical diagnosis of MSA, qualitative imaging features have recently been included as mandatory features [3], underlining their importance. In this analysis, due to the recruitment period, only the former clinical criteria [2] found the basis for the clinical diagnosis of probable MSA-C. We excluded one patient who met these former clinical diagnostic criteria but had an unexpectedly long disease duration of > 30 years. Future studies might be more specific with potentially improved diagnostic accuracy due to the revised clinical criteria. Cerebellar white matter atrophy was pronounced in MSA-C, SCA1 and SCA3, with the steepest and significant decline relative to ataxia severity in SCA3 and MSA-C. In MSA-C, alpha-synuclein deposition in oligodendrocytes represents the central neuropathological changes. However, also

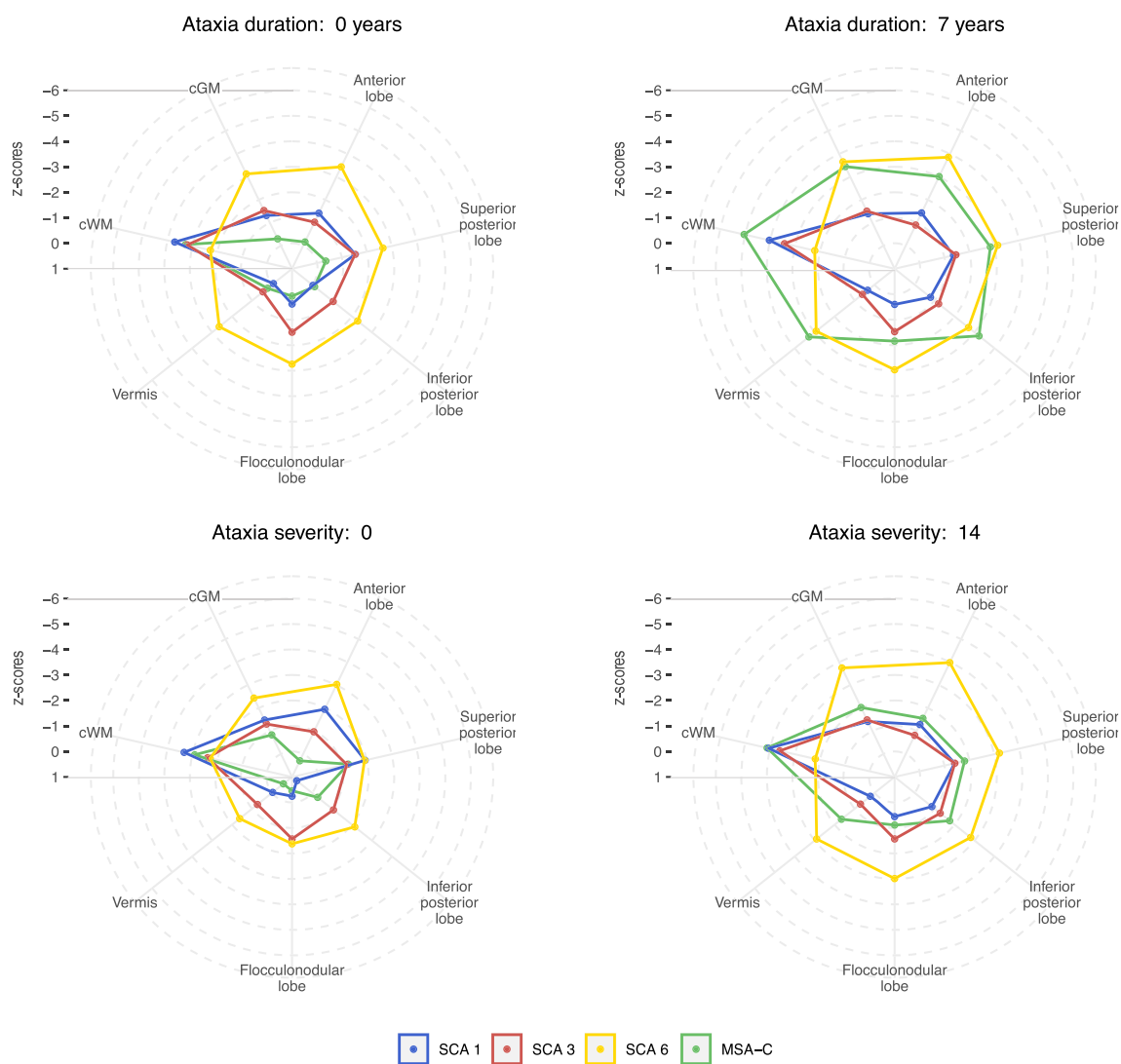


Fig. 4 Radar plot of atrophy in SCA1, SCA3, SCA6 and MSA-C at ataxia duration equal to 0 and 7 years and at ataxia severity of a SARA sum score equal to 0 and 14. For each volume the intercept at an ataxia duration of 0 years (A) as well as the mean ataxia duration of 7 years (B) from the linear interpolation of volume z-scores against ataxia duration, Fig. 2, is given. Similarly, the intercept at SARA sum score of 0

(C) as well as the mean SARA sum score of 14 (D) from the linear interpolation of volume z-scores against ataxia severity, Fig. 3, is given. A z-score of 0 corresponds to the mean of healthy control distribution, while z-scores of ± 1 , ± 2 etc. correspond to values which are 1, 2 etc. standard deviations (SD) of the distributions in HC above or below the mean in HC, respectively

in SCA3 there is increasing evidence for a strong involvement of oligodendrocytes in the disease-specific neuropathology [28].

Our approach allowed the comparison of the different diseases at specific levels of duration and severity of ataxia, yet these results are based on indirect measurements and are therefore subject to limitations that must be considered. The number of available participants, along with their relatively short spans of ataxia duration and severity levels, obviously can impact the linear model. Cubic and quadratic models are provided in the Supplementary Data. However, neither the residual versus fitted values plots nor the Q-Q plots showed

substantial improvement compared to the linear model. Thus, given the limited sample size and previous literature showing linear relations between, e.g., ataxia severity and disease duration [9, 29–31], we kept the linear assumption.

Within the SCAs, in particular SCA1 and SCA3, we found in a minority of volumes a contra-intuitive increase of volumes with increasing ataxia duration or severity. We hypothesise that this is either due to noise or a selection bias with a biased focus on the proportion of less affected patients in advanced stages. Severely affected patients suffer substantial restrictions in mobility and are often no longer able to travel to study visits. Thus, the complete spectrum of

advanced stage patients might not be represented, but rather, there may be a positive selection of those who are still reasonably mobile despite an advanced SARA score. Studies with larger sample sizes and in addition ideally longitudinal data are needed to study the differences between diseases more reliably at comparable levels of ataxia severity and duration. Despite the aforementioned limitations, our results are able to illustrate main principles using comparative visualisations of volumetric changes in cerebellar grey and white matter in MSA-C, SCA1, SCA3 and SCA6 and thereby may inform further studies on a broader data basis.

Conclusion

Application of z-transformation to correct for age effects and the use of a linear model to read-out volumetric values at distinct levels of disease duration and ataxia severity allowed comparison of the extend and pattern of cerebellar atrophy between SCA1, SCA3, SCA6 and MSA-C. In summary, our results confirmed that SCA6 is primarily a pure cerebellar disease with markedly emphasised cGM atrophy. In contrast, a prominent involvement of cWM was found in SCA1, SCA3 and MSA-C. The well-known rapid clinical progression in MSA-C was also reflected in impressive volume loss later in the disease course. Further studies in larger longitudinal samples are needed to confirm our findings and put them on a broader basis.

Supplementary Information The online version contains supplementary material available at <https://doi.org/10.1007/s12311-024-01659-0>.

Acknowledgements TK and BvdW are members of the European Reference Network for Rare Neurological Diseases (ERN-RD, project number 739510). The ESMI consortium acknowledges Ruth Hossinger for the project management of the ESMI project and for all contributions made towards the success of this project. The authors would like to thank Peter Barker for assisting with data collection.

Author Contributions Conception and design of the study: MF, TK, JF; Writing a significant portion of the manuscript: MF, TK, JF; Acquisition and analysis of data: MF, TS, DK, MR, KDH, DT, TME, PG, HGM, BvdW, JvG, JdV, HJ, KMS, GO, JMJ, CO, MP, KR, TK, JF; Figures preparation: MF, JF; All authors reviewed the manuscript.

Funding Open Access funding enabled and organized by Projekt DEAL. This publication is an outcome of ESMI, an EU Joint Programme - Neurodegenerative Disease Research (JPND) project (see www.jpnd.eu). The project is supported through the following funding organisations under the aegis of JPND: Germany, Federal Ministry of Education and Research (BMBF; funding codes 01ED1602A/B); Netherlands, The Netherlands Organisation for Health Research and Development; Portugal, Fundação para a Ciência e Tecnologia (FCT, funding code JPCOFUND/0002/2015); United Kingdom, Medical Research Council For Peer Review (MR/N028767/1). This project has received funding from the European Union's Horizon 2020 research and innovation programme under grant agreement No. 643417. At the US sites this work was in part supported by the National Ataxia Foun-

ation and the National Institute of Neurological Disorders and Stroke (NINDS) grant R01NS080816. The Center for Magnetic Resonance Research is supported by the National Institute of Biomedical Cores for Imaging and Advanced Neuroimaging award P30 NS076408 and S10 OD017974 grant. JF received funding as a fellow of the Hertie Network of Excellence in Clinical Neuroscience. MR is supported by FCT (CEECIND/03018/2018). BvdW from ZonMw, NWO, Gossweiler Foundation, Brugling Fonds, Radboudumc, Hersenstichting. DT received research grants from the Deutsche Forschungsgemeinschaft (DFG), European Union (EU), the Bernd Fink Foundation and the Once Upon a Time Foundation. JJ received grant support from National Institutes of Health (NIH) and Friedrich's Ataxia Research Alliance (FARA).

Availability of Data and Materials This declaration is not applicable.

Declarations

Ethics Approval The study was approved by the local ethics committees. Written informed consent according to the declaration of Helsinki was obtained from all participants.

Conflict of Interest The authors declare no competing interests.

Open Access This article is licensed under a Creative Commons Attribution 4.0 International License, which permits use, sharing, adaptation, distribution and reproduction in any medium or format, as long as you give appropriate credit to the original author(s) and the source, provide a link to the Creative Commons licence, and indicate if changes were made. The images or other third party material in this article are included in the article's Creative Commons licence, unless indicated otherwise in a credit line to the material. If material is not included in the article's Creative Commons licence and your intended use is not permitted by statutory regulation or exceeds the permitted use, you will need to obtain permission directly from the copyright holder. To view a copy of this licence, visit <http://creativecommons.org/licenses/by/4.0/>.

References

1. Klockgether T, Mariotti C, Paulson H. Spinocerebellar Ataxia. *Nat Rev Dis Prim.* 2016;5(1). <https://doi.org/10.1038/s41572-019-0074-3>.
2. Gilman S, Wenning G, Low P, Brooks D, Mathias C, Trojanowski J, et al. Second consensus statement on the diagnosis of multiple system atrophy. *Neurology.* 2008;71(9):670–6. <https://doi.org/10.1212/01.wnl.0000324625.00404.15>.
3. Wenning G, Stankovic I, Vignatelli L, Fanciulli A, Calandra-Buonaura G, Seppi K, et al. Rhe movement disorder society criteria for the diagnosis of multiple system atrophy. *Mov Disord.* 2022;37(6):1131–48. <https://doi.org/10.1002/mds.29005>.
4. Rentiya Z, Hutnik R, Mekkam Y, Bae J. The pathophysiology and clinical manifestations of spinocerebellar Ataxia type 6. *Cerebellum.* 2020;19(3):459–64. <https://doi.org/10.1007/s12311-020-01120-y>.
5. Hernandez-Castillo CR, King M, Diedrichsen J, Fernandez-Ruiz J. Unique degeneration signatures in the cerebellar cortex for spinocerebellar Ataxias 2, 3, and 7. *NeuroImage Clin.* 2018;20:931–8. <https://doi.org/10.1016/j.nicl.2018.09.026>.
6. Reetz K, Costa AS, Mirzazade S, Lehmann A, Juzek A, Rakowicz M, et al. Genotype-specific patterns of Atrophy progression are more sensitive than clinical decline in SCA1, SCA3 and

- SCA6. *Brain*. 2013;136(Pt 3):905–17. <https://doi.org/10.1093/brain/aww369>.
7. Deistung A, Jäschke D, Draganova R, Pfaffenrot V, Hulst T, Steiner KM, et al. Quantitative susceptibility mapping reveals alterations of dentate nuclei in common types of degenerative cerebellar Ataxias. *Brain Commun*. 2022;4(1):fcab306. <https://doi.org/10.1093/braincomms/fcab306>.
 8. Adanyeguh IM, Perlberg V, Henry PG, Rinaldi D, Petit E, Valabregue R, et al. Autosomal dominant cerebellar Ataxias: imaging biomarkers with high effect sizes. *NeuroImage: Clin*. 2018;19:858–67. <https://doi.org/10.1016/j.nicl.2018.06.011>.
 9. Chandrasekaran J, Petit E, Park YW, du Montcel ST, Joers JM, Deelchand DK, et al. Clinically meaningful magnetic resonance endpoints sensitive to Preataxic spinocerebellar Ataxia types 1 and 3. *Ann Neurol*. 2022. <https://doi.org/10.1002/ana.26573>.
 10. Gitaf LLG, Sobreira-Neto MA, Diniz PRB, Éckeli AL, Fernandes RMF, Marques WJ, et al. Voxel-based morphometry and relaxometry demonstrate macro- and microstructural damages in spinocerebellar Ataxia type 3. *Cerebellum*. 2023;22(5):818–24. <https://doi.org/10.1007/s12311-022-01452-x>.
 11. Della Nave R, Ginestroni A, Tessa C, Salvatore E, De Grandis D, Plasmati R, et al. Brain white matter damage in SCA1 and SCA2. An in vivo study using voxel-based morphometry, histogram analysis of mean diffusivity and tract-based spatial statistics. *Neuroimage*. 2008;43(1):10–19. Epub 2008 Jul 11. PMID: 18672073. <https://doi.org/10.1016/j.neuroimage.2008.06.036>.
 12. Faber J, Kügler D, Bahrami E, Heinz LS, Timmann D, Ernst TM, et al. CerebNet: a fast and reliable deep-learning pipeline for detailed cerebellum sub-segmentation. *Neuroimage*. 2022;264:119703. <https://doi.org/10.1016/j.neuroimage.2022.119703>.
 13. Schmitz-Hübisch T, du Montcel ST, Baliko L, Berciano J, Boesch S, Depondt C, et al. Scale for the assessment and rating of Ataxia: development of a new clinical scale. *Neurology*. 2006;66(11):1717–20.
 14. Maas RPPWM, van Gaalen J, Klockgether T, van de Warrenburg BPC. The preclinical stage of spinocerebellar Ataxias. *Neurology*. 2015;85(1):96–103. <https://doi.org/10.1212/WNL.0000000000001711>.
 15. Buckner RL, Head D, Parker J, Fotenos AF, Marcus D, Morris JC, et al. A unified approach for morphometric and functional data analysis in young, old, and demented adults using automated atlas-based head size normalization: reliability and validation against manual measurement of total intracranial volume. *Neuroimage*. 2004;23(2):724–38. <https://doi.org/10.1016/j.neuroimage.2004.06.018>.
 16. Fortin JP, Parker D, Tunc B, Watanabe T, Elliott MA, Ruparel K, et al. Harmonization of multi-site diffusion tensor imaging data. *NeuroImage*. 2017;161:149–70. <https://doi.org/10.1016/j.neuroimage.2017.08.047>.
 17. Fortin JP, Cullen N, Sheline YI, Taylor WD, Aselcioglu I, Cook PA, et al. Harmonization of cortical thickness measurements across scanners and sites. *NeuroImage*. 2018;167:104–20. <https://doi.org/10.1016/j.neuroimage.2017.11.024>.
 18. Johnson WE, Li C. Adjusting batch effects in microarray expression data using empirical Bayes methods. *Biostatistics*. 2007;8(1):118–27. <https://doi.org/10.1093/biostatistics/kxj037>.
 19. R Core Team. R: A language and environment for statistical computing. Vienna; 2023.
 20. Faber J, Schaprian T, Berkan K, Reetz K, França MCJ, de Rezende TJR, et al. Regional brain and spinal cord volume loss in spinocerebellar Ataxia type 3. *Mov Disord*. 2021;36(10):2273–81. <https://doi.org/10.1002/mds.28610>.
 21. Rezende TJR, de Paiva JLR, Martinez ARM, Lopes-Cendes I, Pedrosa JL, Barsottini OGP, et al. Structural signature of SCA3: from presymptomatic to late disease stages. *Ann Neurol*. 2018;84(3):401–8. <https://doi.org/10.1002/ana.25297>.
 22. Eichler L, Bellenberg B, Hahn HK, Köster O, Schöls L, Lukas C. Quantitative assessment of brain stem and cerebellar atrophy in spinocerebellar Ataxia types 3 and 6: impact on clinical status. *AJNR Am J Neuroradiol*. 2011;32(5):890–7. <https://doi.org/10.3174/ajnr.A2387>.
 23. Arruda WO, Meira AT, Ono SE, de Carvalho Neto A, Betting LEGG, Raskin S, et al. Volumetric MRI changes in spinocerebellar Ataxia (SCA3 and SCA10) patients. *Cerebellum*. 2020;19(4):536–43. <https://doi.org/10.1007/s12311-020-01137-3>.
 24. Schulz JB, Borkert J, Wolf S, Schmitz-Hübisch T, Rakowicz M, Mariotti C, et al. Visualization, quantification and correlation of brain atrophy with clinical symptoms in spinocerebellar Ataxia types 1, 3 and 6. *NeuroImage*. 2010;49(1):158–68. <https://doi.org/10.1016/j.neuroimage.2009.07.027>.
 25. Lukas C, Schöls L, Bellenberg B, Rüb U, Przuntek H, Schmid G, et al. Dissociation of grey and white matter reduction in spinocerebellar Ataxia type 3 and 6: a voxel-based morphometry study. *Neurosci Lett*. 2006;408(3):230–235. Epub 2006 Sep 26. <https://doi.org/10.1016/j.neulet.2006.09.007>.
 26. Faber J, Giordano I, Jiang X, Kindler C, Spottke A, Acosta-Cabronero J, et al. Prominent white matter involvement in multiple system Atrophy of cerebellar type. *Mov Disord*. 2020;35(5):816–24. <https://doi.org/10.1002/mds.27987>.
 27. Oender D, Faber J, Wilke C, Schaprian T, Lakghomi A, Mengel D, et al. Evolution of clinical outcome measures and biomarkers in sporadic adult-onset degenerative Ataxia. *Mov Disord*. 2023;38(4):1654–64. <https://doi.org/10.1002/mds.29324>.
 28. Schuster KH, Zalon AJ, Zhang H, DiFranco DM, Stec NR, Haque Z, et al. Impaired oligodendrocyte maturation is an early feature in SCA3 disease pathogenesis. *J Neurosci*. 2022;42(8):1604–17. <https://doi.org/10.1523/JNEUROSCI.1954-20.2021>.
 29. Jacobi H, du Montcel ST, Bauer P, Giunti P, Cook A, Labrum R, et al. Long-term disease progression in spinocerebellar Ataxia types 1, 2, 3, and 6: a longitudinal cohort study. *Lancet Neurol*. 2015;14(11):1101–8. [https://doi.org/10.1016/S1474-4422\(15\)00202-1](https://doi.org/10.1016/S1474-4422(15)00202-1).
 30. Jäschke D, Steiner KM, Chang DI, Claaßen J, Uslar E, Thieme A, et al. Age-related differences of cerebellar cortex and nuclei: MRI findings in healthy controls and its application to spinocerebellar Ataxia (SCA6) patients. *Neuroimage*. 2023;270:119950. <https://doi.org/10.1016/j.neuroimage.2023.119950>.
 31. Oender D, Faber J, Wilke C, Schaprian T, Lakghomi A, Mengel D, et al. Evolution of clinical outcome measures and biomarkers in sporadic adult-onset degenerative ataxia. *Mov Disord*. 2023;38(4):654–64. <https://doi.org/10.1002/mds.29324>.

Publisher's Note Springer Nature remains neutral with regard to jurisdictional claims in published maps and institutional affiliations.

Authors and Affiliations

Mónica Ferreira¹ · Tamara Schaprian¹ · David Kügler¹ · Martin Reuter^{1,2,3} · Katharina Deike-Hoffmann⁴ · Dagmar Timmann⁵ · Thomas M. Ernst⁵ · Paola Giunti^{6,7} · Hector Garcia-Moreno^{6,7} · Bart van de Warrenburg⁸ · Judith van Gaalen^{8,9} · Jeroen de Vries¹⁰ · Heike Jacobi¹¹ · Katharina Marie Steiner⁵ · Gülin Öz¹² · James M. Joers¹² · Chiadi Onyike¹³ · Michal Povazan¹³ · Kathrin Reetz^{14,15} · Sandro Romanzetti¹⁴ · Thomas Klockgether^{1,16} · Jennifer Faber^{1,16}

¹ German Center for Neurodegenerative Diseases (DZNE), Bonn, Germany

² A.A. Martinos Center for Biomedical Imaging, Massachusetts General Hospital, Boston, MA, USA

³ Department of Radiology, Harvard Medical School, Boston, MA, USA

⁴ Department of Neuroradiology, University Hospital Bonn, Bonn, Germany

⁵ Department of Neurology and Center for Translational Neuro- and Behavioral Sciences, University Hospital Essen, University of Duisburg-Essen, Duisburg, Germany

⁶ Ataxia Centre, Department of Clinical and Movement Neurosciences, UCL Queen Square Institute of Neurology, London, UK

⁷ National Hospital for Neurology and Neurosurgery, University College London Hospitals NHS Foundation Trust, London, UK

⁸ Department of Neurology, Donders Institute for Brain, Cognition, and Behaviour, Radboud University Medical Center, Nijmegen, The Netherlands

⁹ Neurology Department, Rijnstate Hospital, Arnhem, The Netherlands

¹⁰ Department of Neurology, University Medical Center Groningen, University of Groningen, Groningen, The Netherlands

¹¹ Department of Neurology, University Hospital Heidelberg, Heidelberg, Germany

¹² Center for Magnetic Resonance Research, Department of Radiology, University of Minnesota, Minneapolis, MN, USA

¹³ Johns Hopkins University School of Medicine, Baltimore, MD, USA

¹⁴ Department of Neurology, RWTH Aachen University, Aachen, Germany

¹⁵ JARA-Brain Institute Molecular Neuroscience and Neuroimaging, Forschungszentrum Jülich, Jülich, Germany

¹⁶ Department of Neurology, University Hospital Bonn, Bonn, Germany